INT. J. HYPERTHERMIA, 1988, VOL. 4, NO. 3, 281–296

Determination of power deposition patterns for localized hyperthermia: a transient analysis

K. B. OCHELTREE† and L. A. FRIZZELL

Bioacoustics Research Laboratory, University of Illinois,
1406 West Green Street, Urbana, Illinois 61801, U.S.A.

(*Received 27 October 1987; accepted 2 June 1987*)

A technique for calculating the power deposition patterns required to maintain a uniform temperature throughout a tumour by application of the steady-state bioheat transfer equation was reported previously. In this paper the previous analysis is extended to define the power deposition patterns that are required to uniformly raise (and maintain) the temperature throughout the tumour to hyperthermic levels. The power deposition patterns are derived from the time-dependent bioheat transfer equation, and analytical results are developed for infinite half-space and spherical tumour models. A three-dimensional numerical method is presented which allows calculation of time-dependent power deposition patterns for arbitrarily shaped tumours. This method is applied to an example of a spherical tumour.

Keywords: hyperthermia, uniform temperature, power deposition, bioheat transfer equation, transient.

1. Introduction

The application of the steady-state bioheat transfer equation to hyperthermia has been the subject of numerous theoretical studies (Cravalho *et al.* 1980, Halac *et al.* 1983, Dickinson 1984, Roemer *et al.* 1984, Strohbehn and Roemer 1984, Ocheltree and Frizzell 1987). The utilization of these studies for actual tumour heating is limited to the period of time after steady-state conditions have been reached, and to other times when a steady-state approximation is applicable. Transient bioheat analysis has typically been limited to models where the heating was constant throughout time and the temperature distributions were allowed to reach steady state (Van Den Berg *et al.* 1983); no additional power deposition was provided at the onset of treatment to raise the tumour temperature to therapeutic levels.

Methods for determining power deposition patterns required to maintain a steady-state uniform tumour temperature have been reported previously (Ocheltree and Frizzell 1987). The steady-state results were derived by considering the bioheat transfer equation with the time-dependent term set to zero:

$$0 = K\nabla^2 T - W_b C_b T + Q_p \tag{1}$$

where K is the thermal conductivity of the tissue (W/m/°C), T is the tissue temperature relative to the arterial blood temperature (°C), W_b is the blood perfusion rate (kg/m^3/s), C_b is the specific heat of blood (J/kg/°C), and Q_p is the local power deposition (W/m^3). The goal was to maintain a uniform elevated temperature T_0, relative to the arterial blood temperature, throughout the tumour under the constraint of zero power

† IBM Corporation, T. J. Watson Research Center, Yorktown Heights, NY 10598

deposition outside the tumour. It was shown that under these conditions a power deposition of

$$Q_p = W_{bt} C_b T_0 \tag{2}$$

was required throughout the tumour volume. The additional subscript 't' indicates values for tumour tissue, which can vary as a function of position.

It was also shown in the same article that the power deposition pattern required to maintain a uniform tumour temperature includes a delta function of power deposition with magnitude P, located at the tumour–normal tissue boundary. For a model consisting of infinite half-spaces of normal and tumour tissue, P is given by

$$P_{hs}^{ss} = T_0 (W_{bn} C_b K_n)^{1/2}, \tag{3}$$

where the superscript 'ss' indicates a steady-state solution, the subscript 'hs' indicates the half-space model, and the subscript 'n' indicates values for the normal tissue surrounding the tumour. For a spherical tumour model with a tumour of radius r_0, the magnitude of the delta function at the tumour boundary is

$$P_s^{ss} = T_0 [(W_{bn} C_b K_n)^{1/2} + K_n / r_0]$$

or

$$P_s^{ss} = P_{hs}^{ss} + T_0 K_n / r_0, \tag{4}$$

where the subscript 's' denotes the spherical model. Additionally, a three-dimensional numerical model was developed to calculate the power deposition pattern required to maintain uniform tumour temperature for arbitrary geometries under steady-state conditions (Ocheltree and Frizzell 1987).

In this paper a time-dependent power deposition pattern which will raise the tumour temperature to the desired steady-state level is determined using the time dependent bioheat transfer equation. This more general solution asymptotically approaches the steady-state solution for large time.

2. Theory

For this investigation the bioheat transfer equation is considered in its time-dependent form:

$$\rho C \frac{dT}{dt} = K \nabla^2 T - W_b C_b T + Q_p, \tag{5}$$

where ρ is the tissue density (kg/m^3), C is the specific heat of the tissue (J/kg/°C), and the other parameters are as defined in eqn (1). As a preliminary step to an analysis using the time-dependent bioheat equation, the applicability of the steady-state solution was examined. This was done by applying the power deposition pattern required to maintain hyperthermic temperatures in the steady-state case, as given by eqn (2), and by calculating the temperature rise with time.

The temperature elevation produced by the steady-state power deposition pattern can be examined by calculating the temperature rise at a point deep within the tumour core where the effects of the surface delta function and heat conduction into surrounding normal tissue can be neglected (note that this assumption is not used in any of the time-dependent analyses that follow this initial calculation). At such a point the gradient of the temperature can be taken as zero, and eqn (5) reduces to

$$\frac{dT}{dt}+\frac{W_{bt}C_bT}{\rho C}=\frac{W_{bt}C_bT_0}{\rho C}. \tag{6}$$

Equation (6) is a first-order nonhomogeneous equation with solution

$$T=T_0[1-\exp(-W_{bt}C_bt/\rho C)]$$

and time constant $\rho C/W_{bt}C_b$. Figure 1 shows a plot of temperature versus time for the tumour core with typical tumour tissue parameters as given in the table. These same tissue parameters are used in all following analyses except where blood perfusion is varied as indicated in the relevant figures. For this example the time required for the temperature to reach 90 per cent of T_0, the steady-state temperature value, is 22 min, a major portion of a hyperthermia session. The obvious conclusion is that the power deposition pattern required to maintain the steady-state temperature is insufficient to raise the tumour temperature to the therapeutic level in a small fraction (for example 10 per cent) of the hyperthermia session. Therefore a solution to the time-dependent bioheat transfer equation must be found involving a time-dependent Q_p.

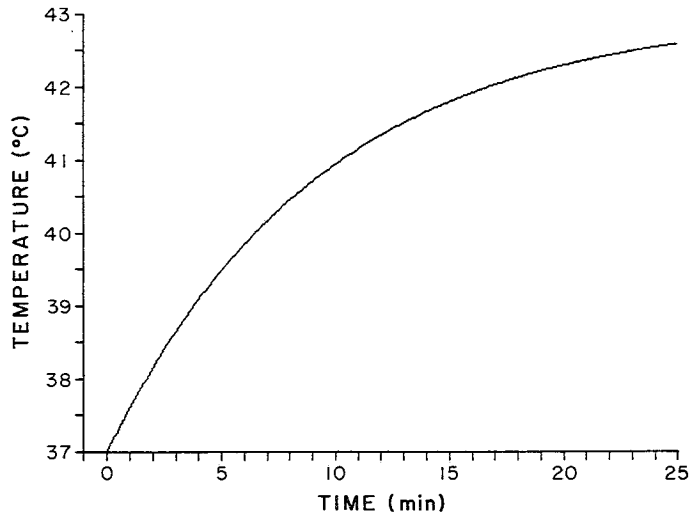

Figure 1. Time dependence of tumour core temperature resulting from application of steady-state power deposition pattern. Heating contribution from power deposition on the tumour periphery has been neglected.

The limitations on Q_p within the tumour for a transient solution are: Q_p must approach $W_{bt}C_bT_0$ (the steady-state solution) for large time, Q_p is non-negative for all

Parameters used for tumour models.

Parameter	Variable	Value
Thermal conductivity	$K(K_n, K_1)$	0·55 W/m/°C
Arterial blood temperature		37·0°C
Blood perfusion rate	$W_b(W_{bn}, W_{bt})$	1·67 kg/m^3/s
Specific heat of blood	C_b	4000 J/kg/°C
Tissue density	ρ	1070 kg/m^3
Specific heat of tissue	C	3500 J/kg/°C
Desired tumour temperature	T_0	6·0°C
Duration of initial heating phase	t_0	360 s

time, and dT/dt is limited by the power that can be supplied by a practical applicator and by the pain associated with increasing temperature too rapidly. Considering the limit on dT/dt, and the simplicity which results from having a constant change of temperature with time within the tumour for the initial heating phase, a desired temperature–time relationship for the entire tumour was chosen as shown in figure 2, with T_0 and t_0 as given in the table. Defining the function $h(t)$ as

$$h(t)=\begin{cases} 0 \text{ for } t\leqslant 0 \\ t \text{ for } 0\leqslant t\leqslant 1, \\ 1 \text{ for } t\geqslant 1 \end{cases} \tag{7}$$

the desired time-dependent temperature can be expressed as

$$T(t)=T_0h(t/t_0). \tag{8}$$

The rate of temperature increase during the initial heating phase is $R=T_0/t_0$ (°C/s).

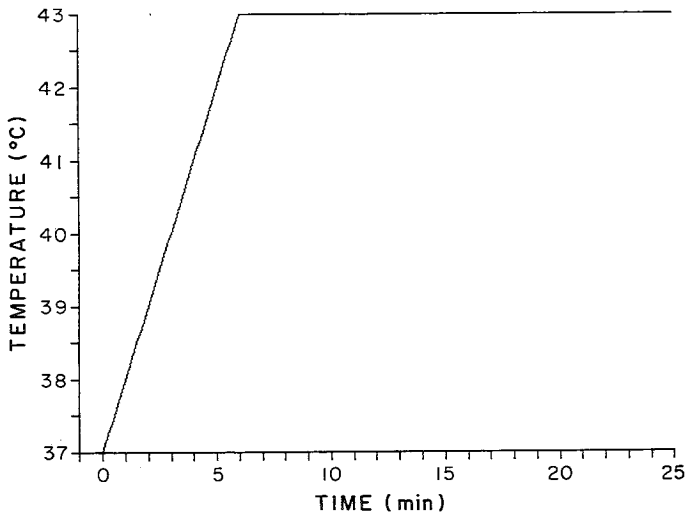

Figure 2. Desired tumour temperature time dependence.

The power deposition required within the tumour to produce the desired transient temperature rise is evaluated by substituting eqn (8) into the time-dependent bioheat transfer equation (eqn (5)). Since the tumour temperature will be raised uniformly, the gradient of the temperature is set to zero to give

$$\rho CR \operatorname{rect}\left(\frac{t-t_0/2}{t_0}\right)=-W_{bt}C_bT_0h(t/t_0)+Q_p, \tag{9}$$

where

$$\operatorname{rect}(t)=\begin{cases} 0 \text{ for } t\leqslant -\frac{1}{2} \\ 1 \text{ for } -\frac{1}{2}\leqslant t\leqslant \frac{1}{2}. \\ 0 \text{ for } t\geqslant \frac{1}{2} \end{cases} \tag{10}$$

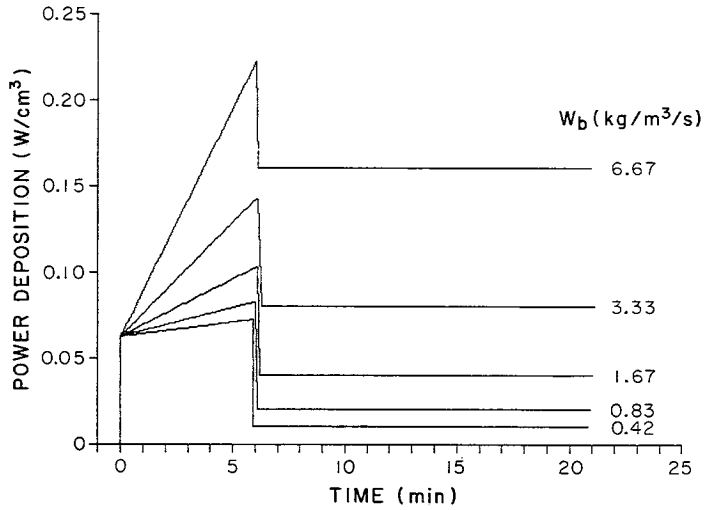

Figure 3. Interior power deposition Q_p time dependence for a range of blood perfusion values.

Solving for Q_p in eqn (9) yields

$$Q_p = W_{bt}C_bT + \rho CR\,\mathrm{rect}\left(\frac{t - t_0/2}{t_0}\right). \tag{11}$$

Figure 3 shows Q_p as a function of time for the tumour parameter values given in the table and a range of blood perfusion rates. From eqn (11) it is seen that Q_p has two terms: the first is equivalent to the steady-state solution (eqn (2)) with T_0 replaced by T, and the second term is equal to ρCR during the initial heating phase and zero thereafter. In this context the significance of each term is apparent: $W_{bt}C_bT$ serves to maintain the achieved elevated temperature by compensating for heat loss due to blood perfusion, while ρCR serves to elevate the temperature at a rate of R degrees per second. The application of eqn (11) is not limited to spatially invariant W_{bt}.

The time varying power deposition pattern within the tumour volume was found to be a function of tissue parameter values, but independent of tumour geometry. In contrast, the power deposition P required on the tumour boundary is a function of tumour shape, and has been determined analytically for two tumour models: an infinite half-space model and a spherical tumour model.

2.1. *Half-space tumour model*

The first tumour model considered consists of two infinite half-spaces: one of homogeneous normal tissue and one of tumour tissue. For such a model the bioheat equation is a function of a single coordinate direction x, and can be simply evaluated to give eqn (11) for the power deposition in the tumour region, $x < 0$. As demonstrated in a previous paper by the authors (Ocheltree and Frizzell 1987), the strength of the power deposition delta function at the tumour boundary is given by

$$P = -K\frac{\mathrm{d}T(x,t)}{\mathrm{d}x}\bigg|_{x=0^-}^{0^+}. \tag{12}$$

This result was derived for the steady-state case, but is applicable to the time-varying

case as well. Thus, in order to determine P, the temperature must be determined for the normal tissue region for all time so that its spatial derivative at $x=0^+$ can be evaluated.

The temperature in the normal tissue region obeys the time-dependent bioheat equation (eqn (5)) with zero power deposition,

$$\rho C\frac{dT}{dt}=K_n\frac{d^2T}{dx^2}-W_{bn}C_bT, \tag{13}$$

subject to the boundary condition

$$T(x=0,t)=T_0h(t/t_0). \tag{14}$$

Evaluation of eqn (13) is lengthy and is included in the Appendix. The time dependence of the temperature distribution for a representative case is shown in figure 4.

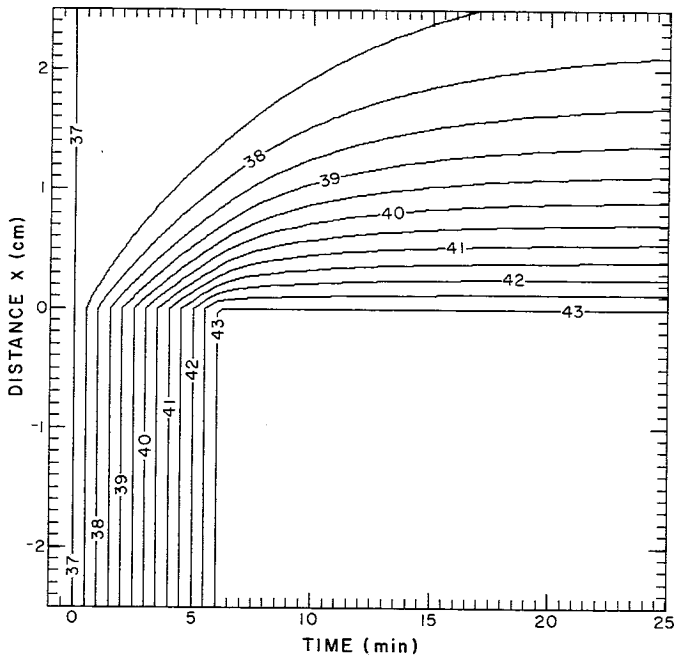

Figure 4. Contour plot of temperature time dependence for a cross-section of the half-space tumour model, tumour ($x<0$) and normal tissue ($x>0$). Temperatures are given at increments of 0·5°C.

The power deposition on the tumour boundary is computed from the temperature distribution using eqn (12). As indicated in the Appendix, the time-dependent power deposition delta function P_{hs}^t is recognized as a function of the steady-state power deposition delta function P_{hs}^{ss} yielding

$$P_{hs}^t=P_{hs}^{ss}\,d(t,t_0,\rho C/W_{bn}C_b), \tag{15}$$

where $d(t,t_0,a)$ is defined as

$$d(t,t_0,a)=\frac{1}{2}+\frac{\sqrt{2}}{\pi t_0}\int_0^\infty\frac{1}{\omega^2}\sin\left(\frac{\omega t_0}{2}\right)\left[((\omega^2a^2+1)^{1/2}+1)^{1/2}\sin\left(\omega\left(t-\frac{t_0}{2}\right)\right)\right.$$
$$\left.+((\omega^2a^2+1)^{1/2}-1)^{1/2}\cos\left(\omega\left(t-\frac{t_0}{2}\right)\right)\right]d\omega. \tag{16}$$

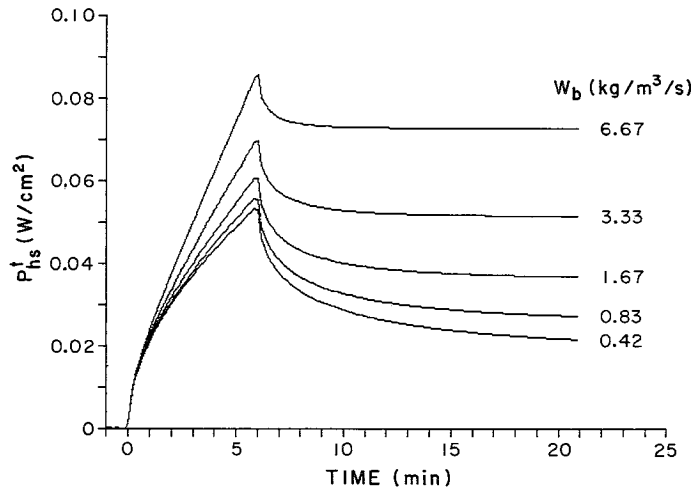

Figure 5. Time dependence of the strength of the delta function required at the tumour boundary for the half-space model, P^t_{hs}, for a range of blood perfusion values.

The function P^t_{hs} is illustrated in figure 5 for typical tumour parameter values and various blood perfusion rates. The differences in the time dependencies of Q_p in the tumour interior and P^t_{hs} can be noted by a direct comparison of figures 3 and 5.

2.2. Spherical tumour model

The second model considered is a spherical tumour of radius r_0 surrounded by an infinitely extended region of homogeneous normal tissue. Despite the infinite extent of the surrounding tissue, the spherical model is applicable to most tumours because heat conduction in the normal tissue is limited to several centimetres when blood perfusion is considered. The temperature and power deposition in the tumour region, $r<r_0$, are again given by eqn (8) and eqn (11), respectively. However, the power deposition delta function at the tumour boundary differs from that for the half-space model due to the curvature of the boundary.

As before, derivation of the power deposition delta function at the tumour boundary requires determination of the temperature in the normal tissue. Outside the tumour, where $r>r_0$, there is no power deposition Q_p and eqn (5) can be expressed in spherical coordinates as

$$\rho C\frac{\partial T}{\partial t}=K_n\frac{\partial^2 T}{\partial r^2}+\frac{2K_n}{r}\frac{\partial T}{\partial r}-W_{bn}C_bT. \tag{17}$$

The derivation of the temperature distribution is provided in the Appendix. The time dependence of this distribution for a 2·5 cm radius tumour model is shown in figure 6. The temperature falls off over a shorter distance for the spherical model (figure 6) than for the half-space model (figure 4) because the heat is conducted outwards in all three coordinate directions rather than in only one.

The strength of the delta function at the tumour periphery (see Appendix) can be expressed in terms of previously defined functions as

$$P^t_s=P^t_{hs}+\frac{T_0K_n}{r_0}h(t/t_0). \tag{18}$$

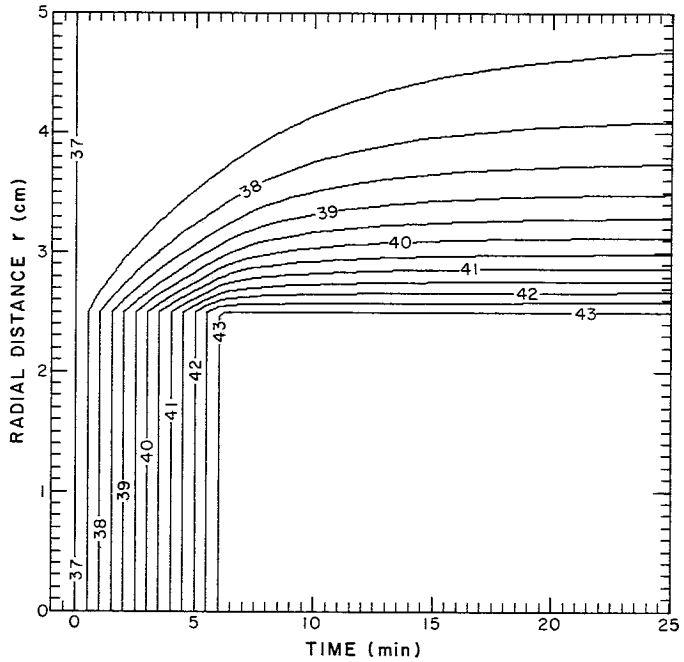

Figure 6. Contour plot of temperature time dependence for a cross-section of the spherical tumour model with 2·5 cm tumour radius, tumour ($r<2{\cdot}5$ cm) and normal tissue ($r>2{\cdot}5$ cm). Temperatures are given at increments of 0·5°C.

A comparison of the time-dependent solution of eqn (18) with the steady-state solution of eqn (4) reveals the similarities of the dependence on tumour radius of the time-dependent and steady-state solutions. The function P_s^t for a tumour radius of 2·5 cm is shown in figure 7 for representative tumour parameters and various blood perfusion rates. More power is required on the periphery of the spherical model (figure 7) that for the half-space model (figure 5) due to the increased heat conducted to the normal tissue.

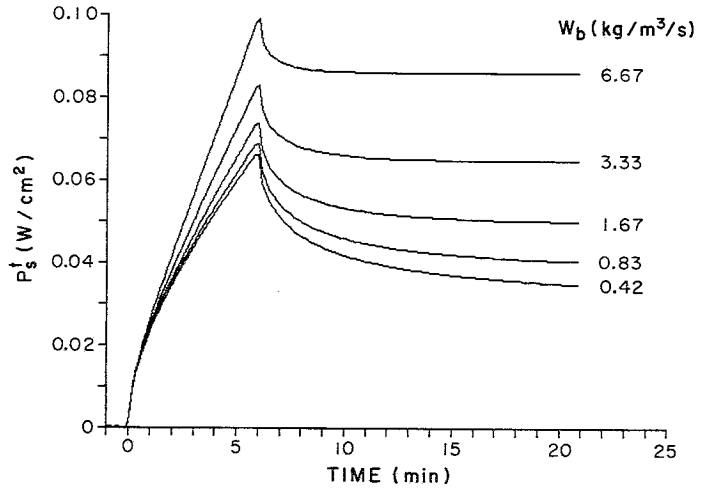

Figure 7. Time dependence of the strength of the delta function required at the tumour boundary for the spherical model, P_s^t, for a range of blood perfusion values. Tumour radius is 2·5 cm.

2.3. *Numerical tumour model*

Applications of the preceding two models are limited to situations where normal tissue parameters are nearly constant and the normal-tumour tissue boundary geometry approaches a spherical shell or a plane. Clearly, a general numerical method, applicable to arbitrarily shaped tumours, would be desirable for clinical applications.

A steady-state numerical method was developed previously (Ocheltree and Frizzell 1987), and has been modified for the calculation of the time-dependent solution. Since the time dependences of the power deposition interior to the tumour and the power delta function at the tumour boundary are different, these regions are handled separately. For a tumour of arbitrary size and shape, eqn (11) holds and specifies the power deposition required at each point interior to the tumour as a function of time. Equation (11) is valid for variable tissue parameters within the tumour as long as a uniform rate of temperature rise R is prescribed throughout the tumour.

The time-dependent power deposition required on the tumour boundary for an arbitrarily shaped tumour with variable tissue properties is related to the steady-state numerical solution. The result represented by eqn (18) can be used by defining an effective tumour radius r_{eff} as the local curvature of the tumour as represented in the numerical model. Denoting the numerical time-dependent solution by P_{n}^{t}, eqn (18) can be rewritten as

$$P_{\text{n}}^{\text{t}} = P_{\text{hs}}^{\text{t}} + \frac{T_0 K_{\text{n}}}{r_{\text{eff}}} h(t/t_0). \tag{19}$$

Taking the limit of eqn (19) as time approaches infinity yields the steady-state numerical power deposition,

$$P_{\text{n}}^{\text{ss}} = P_{\text{hs}}^{\text{ss}} + \frac{T_0 K_{\text{n}}}{r_{\text{eff}}}. \tag{20}$$

Replacing $T_0 K_{\text{n}}/r_{\text{eff}}$ in eqn (19) with its steady-state equivalent from eqn (20) and using eqn (15) gives

$$P_{\text{n}}^{\text{t}} = P_{\text{n}}^{\text{ss}} h(t/t_0) + P_{\text{hs}}^{\text{ss}}[\text{d}(t, t_0, \rho C/W_{\text{bn}} C_{\text{b}}) - h(t/t_0)]. \tag{21}$$

Equation (21) holds for constant tissue properties outside the tumour, and can be used for approximating P_{n}^{t} for nearly constant tissue properties, since P_{n}^{ss} is known and $P_{\text{hs}}^{\text{ss}}$ can be calculated by using the local tissue properties.

The time dependence of the two terms of eqn (21) is shown in figure 8. The first term of eqn (21) increases linearly with time until it reaches the steady-state solution at time t_0, where it remains throughout the duration of the treatment, while the second term increases exponentially to a limit until time t_0, when it begins to decay exponentially to zero. Dependence on the effective tumour radius r_{eff} is not explicitly present, but is incorporated in the numerical steady-state solution P_{n}^{ss}.

3. Results

The numerical solution discussed in the previous section was applied to a spherical tumour model in a three-dimensional rectangular coordinate system. A rectangular coordinate system was used so that an arbitrary tumour geometry could be represented, and a spherical model was chosen for ease of visualization since symmetry assures that a two-dimensional cross-section through the tumour centre is a representative sample. A more complicated tumour geometry could have been chosen, but a complete set of cross-sections would have been required to characterize the power

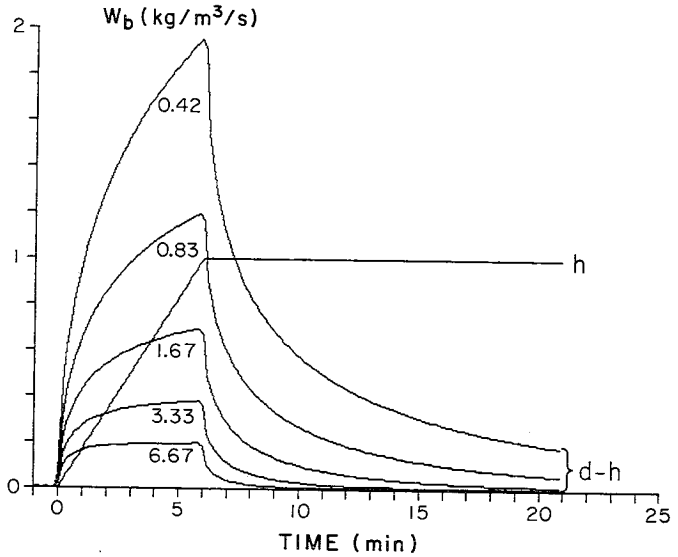

Figure 8. Time dependence of the weighting functions h and $d-h$ for P_n^{ss} and P_{hs}^{ss}, respectively, which are used for the calculation of the numerical delta function strength P_n^t. Weighting functions are shown for a range of blood perfusion values.

deposition pattern at a particular instant in time. Likewise, constant tissue parameters were used to simplify the illustration.

A steady-state numerical solution for a 2 cm radius spherical tumour centred at a depth of 8 cm has been reported previously (Ocheltree and Frizzell 1987). A cross-section of the power deposition pattern required to maintain a constant tumour temperature for this spherical geometry is given in figure 9, along with the resultant temperature distribution. The steady-state numerical solution is used in the determination of the time-dependent solution.

The high power deposition on the periphery of the tumour in figure 9 represents the delta function in the theoretical models, and the variation in the power deposition at the periphery is due to the imperfect representation of the spherical boundary in a rectangular coordinate system. This results in variations in the local curvature of the tumour boundary and the effective radius of the tumour, yielding a varying power deposition on the tumour periphery in accordance with eqn (20).

The power deposition from the steady-state numerical solution, P_n^{ss}, and the steady-state half-space solution as given by eqn (3), P_{hs}^{ss}, are combined with appropriate weighting functions using eqn (21) to give the time-dependent power deposition at the periphery, P_n^t. When this result, P_n^t, is superimposed with the steady-state Q_p weighted as given in eqn (11), the complete numerical time-dependent solution is formed. The time-dependent power deposition required for the case of the spherical tumour is given in figure 10 for several representative times to illustrate the progression of heating required to uniformly raise the tumour temperature to, and maintain it at, a uniform value.

4. Discussion

Results presented here are for the simplified case of constant perfusion with no temperature dependence, an over-simplification that yields demonstrative results that are impractical for direct applications. The numerical method can be modified to

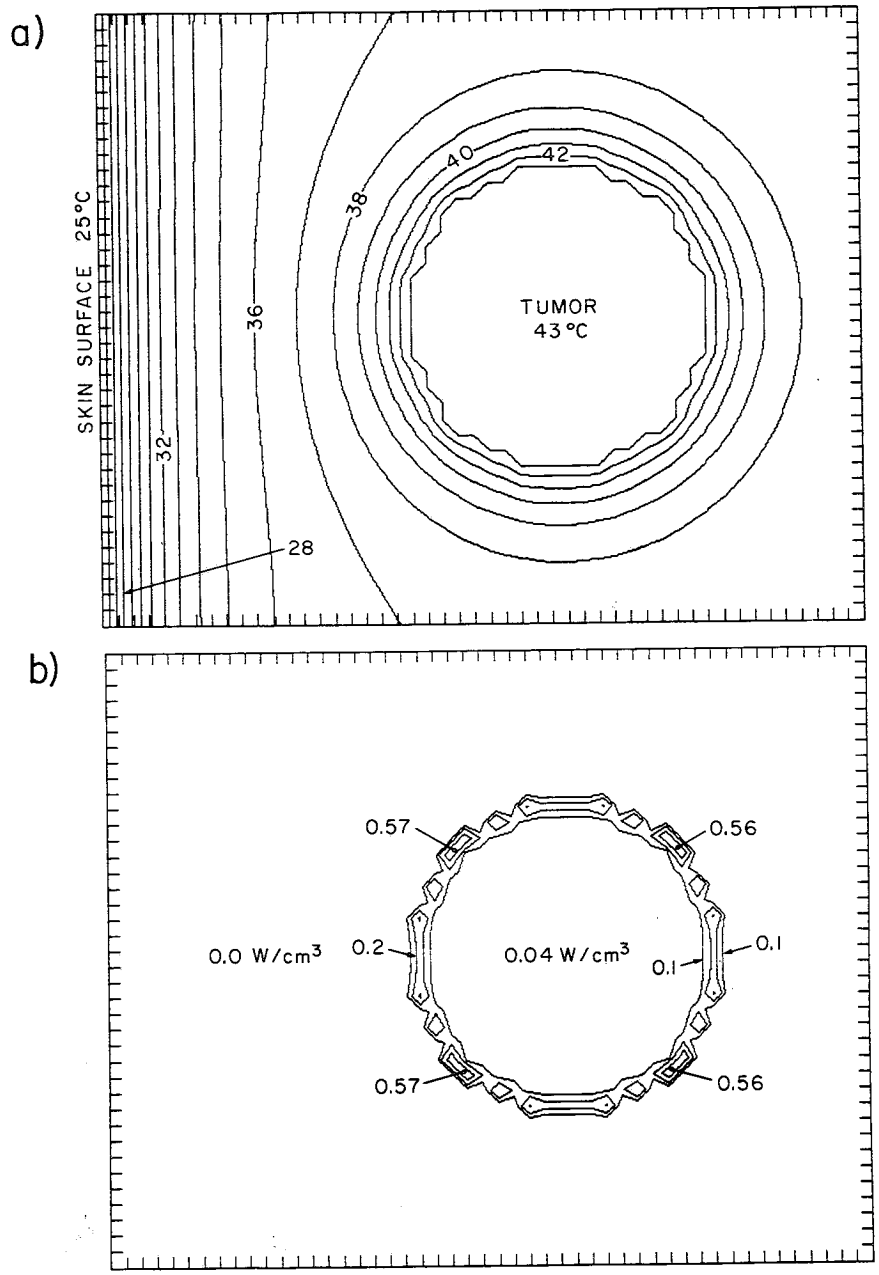

Figure 9. Contour plots of a cross-section of the temperature (*a*) and power deposition (*b*) distributions for a numerically calculated spherical tumour model sampled every 2 mm under steady-state conditions. Temperature contours are shown for 1°C increments and power deposition contours are given for 0·1 W/cm^3, 0·2 W/cm^3, and 0·4 W/cm^3.

incorporate the additional complications that arise in practical applications, though only an approximation to the spatial distribution of blood flow is likely to be available.

The power deposition patterns derived in this study are ideal, and cannot be formed exactly with real applicators; however, they can be used to provide a goal for efficient tumour heating. The material presented in this paper is useful for two purposes: to give

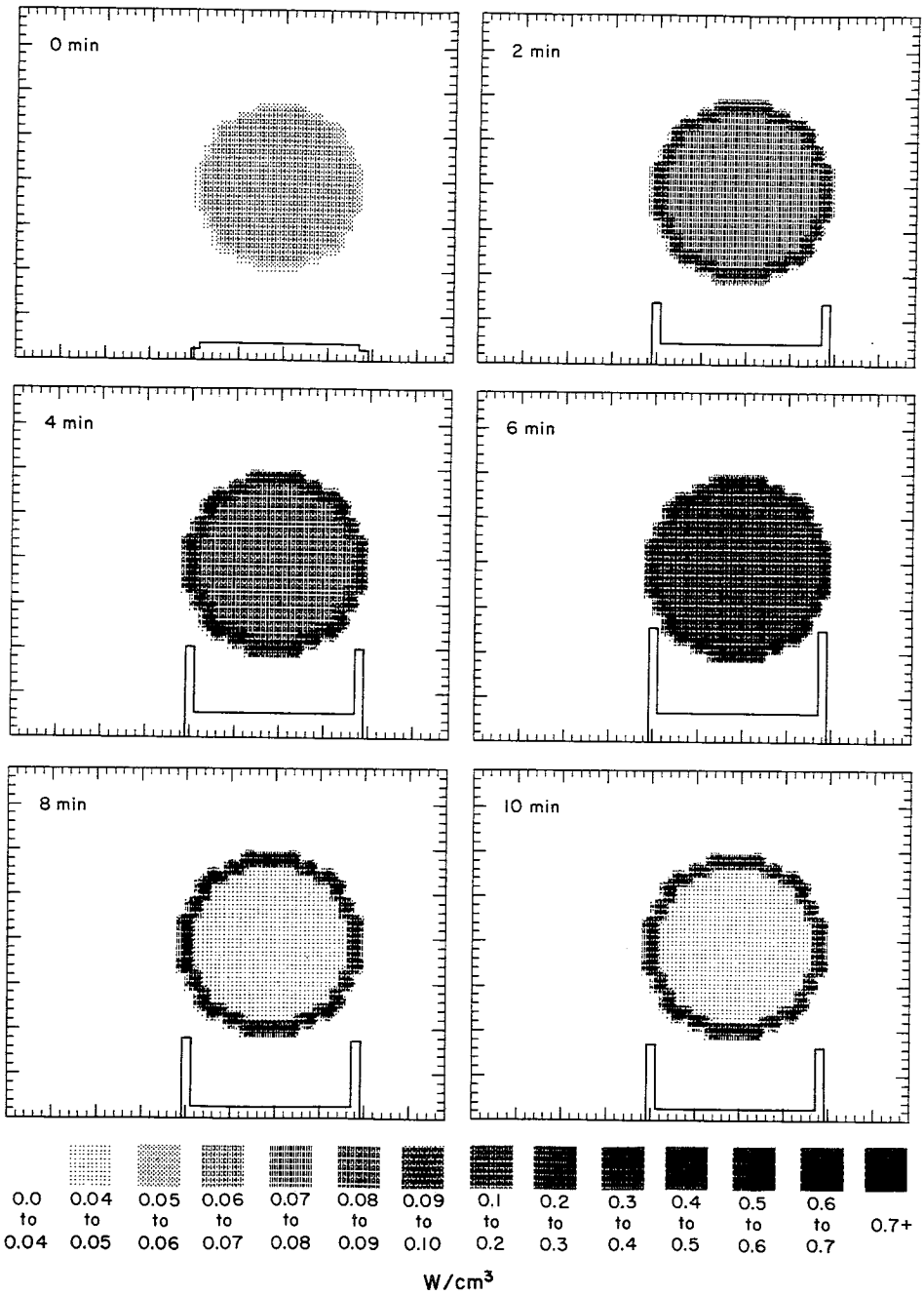

Figure 10. Grey scale plots of a cross-section of the power deposition for a numerically calculated spherical tumour model sampled every 2 mm with major divisions indicated every centimetre. Cross-sections are shown for times of 0, 2, 4, 6, 8 and 10 min. The skin surface is located at the left side of each cross-section and the tumour is centred at a depth of 8 cm. Corresponding power profiles taken along a line through the skin surface and tumour centre are presented with each cross-section.

an understanding of the time-dependent power deposition required to achieve and maintain a uniform therapeutic temperature, and to yield a numerical model that can be adapted for clinical usage. The results indicate that a more uniform power deposition pattern is desirable for raising the temperature to the therapeutic level, while the power deposition pattern with elevated power at the periphery of the tumour is more suitable for maintaining steady-state. Attempting to raise the temperature by simply elevating the power levels sufficient for maintaining steady-state will cause the temperature rise of the interior region to lag behind that of the peripheral regions of the tumour.

Such a detailed analysis of the power deposition patterns that produce desired temperatures within the tumour is necessary to yield insight into how precision hyperthermia applicators can best be utilized. The results presented show that different power deposition patterns are necessary during the initial heating and the steady-state periods of hyperthermia. Practical applications of this theoretical material have been considered, and are treated in a separate paper (Ocheltree and Frizzell 1988).

Acknowledgments

This study was supported in part by Labthermics Technologies, Inc., and in part by a fellowship from the Caterpillar Corporation. The authors are thankful to R. L. Magin and J. F. McCarthy for helpful discussions.

Appendix

A.1. *Half-space solution*

The solution of eqn (13) subject to the condition given in eqn (14) is possible because eqn (13) is separable in x and t. Assuming that $T(x, t)$ can be expressed as a summation of separable eigenfunctions of the form $v(t)u(x)$, and using a separation constant of $j\omega\rho C$ for eqn (13), yield

$$v(t)=e^{j\omega t}$$

and

$$u(x)=e^{-(f+jg)x},$$

where

$$f+jg=[(W_{bn}C_b/K_n)+(j\omega\rho C/K_n)]^{1/2} \tag{A 1}$$

Evaluating the square root of eqn (A 1) so that $u(x)$ remains finite as x approaches positive infinity gives

$$f=\left\{\frac{W_{bn}C_b}{2K_n}\left[\left(\frac{\omega^2\rho^2C^2}{W_{bn}^2C_b^2}+1\right)^{1/2}+1\right]\right\}^{1/2} \tag{A 2}$$

$$g=\frac{\omega}{|\omega|}\left\{\frac{W_{bn}C_b}{2K_n}\left[\left(\frac{\omega^2\rho^2C^2}{W_{bn}^2C_b^2}+1\right)^{1/2}-1\right]\right\}^{1/2} \tag{A 3}$$

The general form of the temperature can then be expressed as the integral over all eigenfunctions:

$$T(x,t)=\int_{-\infty}^{\infty}A(\omega)e^{-(f+jg)x}e^{j\omega t}\,d\omega, \tag{A 4}$$

where $A(\omega)$ is a constant dependent on the boundary conditions. To determine $A(\omega)$,

eqn (A 4) is evaluated at $x=0$ so that the boundary conditions of eqn (14) can be applied

$$T(x=0,t)=\frac{1}{2\pi}\int_{-\infty}^{\infty}2\pi A(\omega)e^{j\omega t}\,d\omega. \tag{A 5}$$

Equation (A 5) is recognized as the expression of an inverse Fourier transform, so that

$$A(\omega)=\frac{1}{2\pi}F\{T(x=0,t)\}, \tag{A 6}$$

where F denotes the Fourier transform. Substituting eqn (14) into eqn (A 6) yields

$$A(\omega)=\frac{1}{2\pi}F\{T_0h(t/t_0)\},$$

or equivalently

$$A(\omega)=\frac{1}{2\pi}F\left\{\int_{-\infty}^{t}\frac{T_0}{t_0}\,\mathrm{rect}\left(\frac{\tau-t_0/2}{t_0}\right)d\tau\right\} \tag{A 7}$$

The Fourier transform in eqn (A 7) can be evaluated using transform tables (Stremler 1977) to yield

$$A(\omega)=\frac{T_0}{j\pi\omega^2t_0}\sin\left(\frac{\omega t_0}{2}\right)e^{-j\omega t_0/2}+\frac{T_0}{2}\delta(\omega).$$

Substituting this result into eqn (A 4) and reducing yields a general expression for T in the region $x>0$,

$$T(x,t)=\frac{T_0}{2}e^{-(W_{bn}C_b/K_n)^{1/2}x}+\frac{2T_0}{\pi t_0}\int_0^{\infty}\frac{e^{-fx}}{\omega^2}\sin\left(\frac{\omega t_0}{2}\right)\sin\left[\omega\left(t-\frac{t_0}{2}\right)-gx\right]d\omega. \tag{A 8}$$

This integral was computed numerically to give the time-dependent temperature distribution shown in figure 4.

The power deposition delta function at the tumour boundary is determined by substituting eqn (A 8) into eqn (12) and evaluating to yield

$$P_{hs}^{t}=\frac{T_0}{2}(W_{bn}C_bK_n)^{1/2}+\frac{2K_nT_0}{\pi t_0}\int_0^{\infty}\frac{1}{\omega^2}\sin\left(\frac{\omega t_0}{2}\right)\left\{f\sin\left[\omega\left(t-\frac{t_0}{2}\right)\right]+g\cos\left[\omega\left(t-\frac{t_0}{2}\right)\right]\right\}d\omega$$

where the superscript 't' indicates the time-dependent solution. Comparing this result with eqn (3) gives

$$P_{hs}^{t}=P_{hs}^{ss}\left\{\frac{1}{2}+\frac{\sqrt{2}}{\pi t_0}\int_0^{\infty}\frac{1}{\omega^2}\sin\left(\frac{\omega t_0}{2}\right)\left[\left[\left(\frac{\omega^2\rho^2C^2}{W_{bn}^2C_b^2}+1\right)^{1/2}+1\right]^{1/2}\sin\left[\omega\left(t-\frac{t_0}{2}\right)\right]+\left[\left(\frac{\omega^2\rho^2C^2}{W_{bn}^2C_b^2}+1\right)^{1/2}-1\right]^{1/2}\cos\left[\omega\left(t-\frac{t_0}{2}\right)\right]\right]d\omega\right\}.$$

A.2. *Spherical solution*

Again, $T(x,t)$ is assumed to be expressible as the summation of separable eigenfunctions of the form $v(t)u(r)$. Using a separation constant of $j\omega\rho C$, gives

$$v(t)=e^{j\omega t}$$

and

$$u(r)=\frac{e^{-(f+jg)r}}{r}$$

where f and g are given by eqn (A 2) and eqn (A 3), respectively. The general form of the temperature is

$$T(r,t)=\int_{-\infty}^{\infty}\frac{A(\omega)}{r}e^{(f+jg)r}e^{j\omega t}\,d\omega,$$

which is evaluated at $r=r_0$ for application of the boundary condition to give

$$T(r_0,t)=\frac{1}{2\pi}\int_{-\infty}^{\infty}\frac{2\pi A(\omega)}{r_0}e^{(f+jg)r_0}e^{j\omega t}\,d\omega. \tag{A 9}$$

Equation (A 9) has the form of an inverse Fourier transform and can be evaluated using the same method as for the half-space model to yield

$$T(r,t)=\frac{T_0 r_0}{2r}e^{-(W_{bn}C_b/K_n)^{1/2}(r-r_0)}$$
$$+\frac{2T_0 r_0}{\pi t_0 r}\int_0^{\infty}\frac{1}{\omega^2}e^{-f(r-r_0)}\sin\left(\frac{\omega t_0}{2}\right)\sin\left[\omega\left(t-\frac{t_0}{2}\right)-g(r-r_0)\right]d\omega. \tag{A 10}$$

The strength of the delta function at the tumour periphery is

$$P=-K\frac{dT(r,t)}{dr}\bigg|_{r=r_0-}^{r_0+}. \tag{A 11}$$

Substituting eqn (A 10) into eqn (A 11) and reducing yields

$$P_s^t=\frac{T_0}{2}(W_{bn}C_bK_n)^{1/2}+\frac{T_0K_n}{2r_0}+\frac{2K_nT_0}{\pi t_0}\int_0^{\infty}\frac{1}{\omega^2}\sin\left(\frac{\omega t_0}{2}\right)$$
$$\times\left\{\left(f+\frac{1}{r_0}\right)\sin\left[\omega\left(t-\frac{t_0}{2}\right)\right]+g\cos\left[\omega\left(t-\frac{t_0}{2}\right)\right]\right\}d\omega.$$

This can be further reduced and expressed in terms of previously defined functions as

$$P_s^t=P_{hs}^t+\frac{T_0K_n}{r_0}h(t/t_0).$$

References

CRAVALHO, E. G., FOX, L. R., and KAN, J. C., 1980, The application of the bioheat equation to the design of thermal protocols for local hyperthermia. *Annals of the New York Academy of Sciences*, **335**, 86–97.

DICKINSON, R. J., 1984, An ultrasonic system for local hyperthermia using scanned focused transducers. *IEEE Transactions Biomedical Engineering*, **31**, 120–125.

HALAC, S., ROEMER, R. B., OLESON, J. R., and CETAS, T. C., 1983, Magnetic induction heating of tissue: Numerical evaluation of tumour temperature distributions. *International Journal of Radiation Oncology, Biology, and Physics*, **9**, 881–891.

OCHELTREE, K. B., and FRIZZELL, L. A., 1987, Determination of power deposition patterns for localized hyperthermia: a steady-state analysis. *International Journal of Hyperthermia*, **3**, 269–279.

OCHELTREE, K. B., and FRIZZELL, L. A., 1988, Applicator configurations and scan paths for localized hyperthermia (in preparation).

ROEMER, R. B., SWINDELL, W., CLEGG, S. T., and KRESS, R. L., 1984, Simulation of focused, scanned ultrasonic heating of deep-seated tumors: the effect of blood perfusion. *IEEE Transactions on Sonics and Ultrasonics*, **31**, 457–466.

STREMLER, F. G., 1977, *Introduction to Communication Systems* (Reading, Mass.: Addison-Wesley), pp. 75–100.

STROHBEHN, J. W., and ROEMER, R. B., 1984, A survey of computer simulations of hyperthermia treatments. *IEEE Transactions on Biomedical Engineering*, **31**, 136–149.

VAN DEN BERG, P. M., DE HOOP, A. T., SEGAL, A., and PRAAGMAN, N., 1983, A computational model of the electromagnetic heating of biological tissue with application to hyperthermic cancer therapy. *IEEE Transactions on Biomedical Engineering*, **30**, 797–805.